Finite Time Fault Tolerant Control for Robot Manipulators Using Time Delay Estimation and Continuous Nonsingular Fast Terminal Sliding Mode Control

Mien Van, Shuzi Sam Ge, *Fellow*, *IEEE,* Hongliang Ren, *Member, IEEE*

***Abstract*— In this paper, a novel finite time fault tolerant control (FTC) is proposed for uncertain robot manipulators with actuator faults. First, a finite time passive fault tolerant control (PFTC) based on a robust nonsingular fast terminal sliding mode control (NFTSMC) is investigated. Be analyzed for addressing the disadvantages of the PFTC, the AFTC are then investigated by combining NFTSMC with a simple fault diagnosis (FD) scheme. In this scheme, an online fault estimation algorithm based on time delay estimation (TDE) is proposed to approximate actuator faults. The estimated fault information is used to detect, isolate and accommodate the effect of the faults in the system. Then, a robust AFTC law is established by combining the obtained fault information and a robust NFTSMC. Finally, a high-order sliding mode (HOSM) control based on super-twisting algorithm is employed to eliminate the chattering. Compared to the PFTC and other state-of-the-art approaches, the proposed AFTC scheme possess several advantages such as high precision, strong robustness, no singularity, less chattering and fast finite-time convergence due to the combined NFTSMC and HOSM control, and requires no prior knowledge of the fault due to TDE-based fault estimation. Finally, simulation results are obtained to verify the effectiveness of the proposed strategy.**

***Index Terms*—Fault diagnosis, fault tolerant control, time delay estimation, terminal sliding mode, robot manipulators.**

I. Introduction

NOWADAY, robotic technologies have been widely applied for real applications such as in military, industry, medicine, productivity, reliability, etc. However, applications that require robots to be placed in hazardous, remote environment and interaction with humans can lead to robot failure, which could degrade product quality and endanger users and other objects in the workspace. Hence, automated monitoring-diagnostics of the robotic system play a crucial role for the use of robotic manipulators as parts of autonomous system. In addition, in dangerous or remote environments, it is difficult to repair the failed robot. Thus, it is important to develop a control scheme to guarantee that a robot can continue to reliably work in the presence of faults.

Due to the aforementioned requirement, various fault diagnosis (FD) approaches for robotic systems have been studied over the last three decades. In the literature, model-based analytical redundancy-based fault detection and isolation have been investigated [1-3]. Using intelligent learning techniques such as neural network (NN) or fuzzy logic, robust FD methods have also been proposed [4-10].The basic idea of these methods is to design a robust FD scheme using a model-based method and then use the NN [4-7] or fuzzy logic [8-10] to approximate the faults in the observer design. The intelligent learning techniques have the capability to approximate the unknown fault functions in robot dynamics; however, they introduce a number of weighting parameters or fuzzy rules that make implementation difficult and time consumption. Due to its inherent robustness to system uncertainties and external disturbances [11], sliding mode observer has been used in the design of fault diagnostic observers [12-15]. Although this technique is simple in design and has a fast convergence; however, the design system requires a prior knowledge of bounded faults, which could be, from a practical point of view, hard to acquire. In robotic system, faults usually occur at unknown time and with unknown magnitude. To relax the requirement of bounded faults of sliding mode observer, neural sliding mode observers, which combine the NN and the sliding mode observers, have been developed in our previous studies [16-17]. However, these approaches still contain the intelligent learning technique; it may meet, as aforementioned, a difficulty in real implementation. Time delay estimation (TDE) technique developed in [18-19] is a simple but robust technique to approximate a nonlinear function without prior knowledge on bounded unknown input by using time delay information. This technique has been successfully used to approximate the unknown dynamic model of robot manipulators [20-22]. However, to the best of our knowledge, there is no study in literature on the use of TDE to carry out robust fault diagnosis.

Mien Van, Shuzi Sam Ge, Hongliang Ren, are with the Faculty of Engineering & Advanced Robotic Centre, National University of Singapore, 117580, Singapore (e-mail: {bievm, ren,ge}@nus.edu.sg).

In some applications that require robot to be worked in dangerous or remote environment, it is required that a fault should be automatically self-corrected after it is detected and isolated so as to enhance the system reliability and guarantee the control performance. This task is referred to as fault-tolerant control (FTC). In general, FTC systems can be divided into two categories: active and passive approaches [23-24]. In passive FTC (PFTC) systems, one controller is used for both the normal case and the fault case without the need to detect the presence of a fault [25-28]. However, this approach requires partial knowledge of a possible system fault, so its use is limited in real applications. In contrast, active FTC (AFTC) is designed based on fault information [3-9, 29-33]. FD is the first step to provide the fault information. The AFTC scheme is then designed based on the obtained fault information in order to compensate for the effect of a fault in the system. For this reason, the system performance of the AFTC depends on the accuracy of the fault information that has been obtained. With the correct fault information, the performance of AFTC system is more effective than that of a PFTC, and hence, is more desirable for practical applications.

Although many FTC schemes have been developed in the literature for various linear and nonlinear systems, to the best knowledge of the authors, there have been only minor FTC investigations for robotic systems with fast finite time convergence. In fact, most of the developed FTC schemes for robot manipulators are designed based on modification of the nominal computed torque controller (CTC) [4-8, 16-17]. The basic idea behind these approaches is to use a CTC along with estimated fault compensation based on learning techniques. However, as aforesaid, the use of learning methods has a difficulty in real implementation. On the other hand, the use of CTC as a nominal controller has two major drawbacks in real robot applications. Firstly, it requires an exact model of the robot dynamics, which is usually challenging. Secondly, it is not robust to structured and unstructured uncertainties, which may result in poor performance. Therefore, these approaches do not compensate for the modeling uncertainty when designing the nominal controller for normal operation, although the uncertainty can be compensated when a fault occurs. Consequently, the tracking performance is decreased. Many advanced control approaches have been proposed to increase the performance of the robot system for normal operation, such as adaptive control [34-35], fuzzy control [36-37], neural network control [38-39], optimal control [40] and sliding mode control (SMC) [41-42], etc.

Compared to other methods, SMC has attractive advantages of robustness to uncertainties and disturbances and low sensitivity to the system parameter variations [10, 43]. This technique has been used for the design of FTC system [44-45]. However, the uses of traditional SMC scheme do not converge to the equilibrium point in finite time because a linear surface is used. Recently, terminal sliding mode control (TSMC) methods [46-47], which use nonlinear sliding surfaces instead of linear surfaces, have been developed. By suitably designing the parameters, the TSMC assures the system states to reach the equilibrium point in finite time, and also offers some superior properties such as rapid response, robustness and higher precision. However, the initial TSMC has two disadvantages: the first is that it has slower convergence to the equilibrium than the traditional linear sliding mode control when the system state is far away from the equilibrium, and the second is the singularity problem. To overcome the first disadvantage of the traditional TSM, fast terminal sliding mode (FTSM) control has been developed [48-49]; however, these approaches still have a singular problem. In order to eliminate the singular problem, nonsingular TSMC (NTSMC) [50-53] and nonsingular fast terminal sliding mode control (NFTSMC) [54-57] have been proposed. Compared to the NTSMC, the NFTSMC has the same property but provides a faster state convergence. However, both SMC and TSMC techniques have a drawback that they produce the high-frequency oscillations of the controller output, known as chattering. In practical implementations, chattering is undesirable because it may excite unmodelled high frequency plant dynamics resulting in unforeseen instabilities. To remove the chattering, several solutions have been proposed. One solution is to use the boundary layer method that includes *sigmoid* function [56] or *saturation* function [58] instead of *sign* function. This approach, however, can only guarantee the existence condition of the sliding mode outside a small boundary layer around the sliding manifold, which will increase the steady state tracking errors. A second solution is to design of a continuous control law [49, 57]. However, this technique implies deterioration accuracy and/or robustness. A third solution proposed to decrease the chattering is the high-order sliding mode (HOSM) technique [59-66]. Unlike the SMC, which works on the first time derivative of the sliding mode variable, HOSM works with discontinuous control acting on the high-order time derivative. By moving the switching to the higher derivatives of the control, the control signal becomes continuous, so the chattering is much reduced.

In light of the remarkable benefits and limitations, this paper investigates a finite time AFTC scheme for uncertain robot manipulator based on TDE and NFTSMC combined with a HOSM control technique so as to accommodate both the uncertainties and faults. To highlight the benefits of the proposed AFTC, the PFTC based on NFTSMC is first presented; and its benefits and limitations are analyzed. Then, based on the limitations, the AFTC based on NFTSMC and TDE is then proposed. In this scheme, TDE is proposed as a robust FD scheme to approximate the fault information; the obtained fault information is used to detect, isolate and accommodate the effects of faults. Then, NFTSMC is used to compensate for the TDE error and stabilize the control system. Finally, a super-twisting HOSM algorithm is employed to eliminate the chattering.

Comparing to the existing approaches, the contribution of this paper can be marked as the following significant points:

- Unlike the intelligent learning techniques or sliding mode observer, TDE- based FD scheme is proposed for the first time.
- A novel fast finite time AFTC scheme is proposed based on the combining of TDE-based fault diagnosis and NFTSMC and HOSM controllers.
- The proposed FTC system considers and compensates for the effects of both the uncertainty and fault in both healthy and fault operations.
- The proposed FTC scheme possess several advantages over other state-of-the-art approaches such as higher precision, robustness, no singularity, less chattering, fast finite time convergence and no need for prior knowledge of bounded faults.

The rest of this paper is organized as follows. Section II formulates the problem and gives preliminaries. Section III and IV introduce the design of proposed PFTC based on NFTSMC and proposed AFTC based on NFTSMC and TDE, respectively. The simulation results for a PUMA560 robot are given in section V so as to verify the effectiveness of the proposed algorithms. Finally, the conclusions are given in Section VI.

II. Problem Statement and Premilinaries

A. Problem statement

Consider the robot dynamics described by

$$\begin{aligned}\ddot{q} = M^{-1}(q)\big(\tau - V_m(q,\dot{q})\dot{q} - F(\dot{q}) - G(q) - \tau_d\big) \\ + \gamma(t-T_f)\phi(q,\dot{q},\tau)\end{aligned} \tag{1}$$

where $q \in \Re^n$ is the state vector, $\tau \in \Re^n$ is the torque produced by the actuators, $M(q) \in \Re^{nxn}$ is the inertia matrix, $V_m(q,\dot{q}) \in \Re^n$ includes the Coriolis and centripetal forces, $F(\dot{q}) \in \Re^n$ is the friction matrix, τ_d is a load disturbance matrix and $G(q) \in \Re^n$ is the vector of gravity terms. The term $\phi(q,\dot{q},\tau) \in \Re^n$ is a vector representing the faults, $\gamma(t-T_f) \in \Re^n$ represents the time profile of the faults, and T_f is the time of occurrence of the faults.

The robot dynamics (1) have the following standard properties. The inertia matrix $M(q)$ is symmetric positive define, and

$$0 < \lambda_m\{M(q)\} \le \|M\| \le \lambda_M\{M(q)\} \le \chi, \quad \chi > 0 \tag{2}$$

where $\lambda_M\{M\}$ and $\lambda_m\{M\}$ are the maximum and minimum eigenvalues of matrix M .

We let the time profile $\gamma(\cdot)$ be a diagonal matrix of the form

$$\gamma(t-T_f) = diag\{\gamma_1(t-T_f), \gamma_2(t-T_f), \ldots, \gamma_n(t-T_f)\} \tag{3}$$

where γ_i is a fault function that represents the fault affecting the *i*th state equation.

The faults with time profiles modeled are given by

$$\gamma_i(t-T_f) = \begin{cases} 0 & if\ t < T_f \\ 1 - e^{-\psi_i(t-T_f)} & if\ t \ge T_f \end{cases} \tag{4}$$

where $\psi_i > 0$ represents the unknown fault evolution rate. A small value of ψ_i characterizes a slowly developing fault, also called an incipient fault. For a large value of φ_i, the profile of γ_i approaches a step function that models abrupt faults. When $\psi_i \to \infty$, γ_i becomes a step function so that the incipient fault becomes an abrupt fault.

In this paper, actuator faults are considered because it represents one of the most serious failures and usually occurs in robotic systems. In a robotic system, damage to the actuators can be caused by damage to an internal actuator, the power supply systems, or wirings, etc. This class of failure can be described by the difference between the nominal torque τ_0 and the actuator τ acting at the robot joint; it can be expressed as:

$$\tau(t) = \tau_0(t) + \delta\tau(t) \tag{5}$$

The actuator fault $\delta\tau(t)$ can be represented by the fault function $\phi(q,\dot{q},\tau)$ in (1) as: $\phi(q,\dot{q},\tau) = M^{-1}(q)\delta\tau(t)$.

To simplify the design in the next section, the robot dynamics can be rewritten as

$$\begin{aligned}\ddot{q} &= M^{-1}(q)\tau + M^{-1}(q)\big[-V_m(q,\dot{q})\dot{q} - G(q)\big] \\ &\quad + M^{-1}(q)\big[-F(\dot{q}) - \tau_d\big] + \gamma(t-T_f)\phi(q,\dot{q},\tau) \\ &= M^{-1}(q)\tau + f(q,\dot{q}) + \Delta(q,\dot{q},\tau) + \gamma(t-T_f)\phi(q,\dot{q},\tau)\end{aligned} \tag{6}$$

where $f(q,\dot{q}) = M^{-1}(q)\big[-V_m(q,\dot{q})\dot{q} - G(q)\big]$ represents the known nominal robot dynamics and $\Delta(q,\dot{q},\tau) = M^{-1}(q)\big[-F(\dot{q}) - \tau_d\big]$ represents the uncertainties in the nominal model.

The objective of this paper is twofold: *i*) design a FD scheme to detect, isolate and estimate the fault $\phi(q,\dot{q},\tau)$; and *ii*) design a fast finite time AFTC scheme based on the obtained fault information such that the system outputs can follow the desired trajectories well in the presence of both uncertainty and fault.

B. Notations

$x^{[c]} = |x|^c \, sign(x)$, where $c > 0$

It can be easily verified that as $c \geq 1$

$$\frac{d}{dt}x^{[c]} = c|x|^{c-1}\dot{x}$$

The *sign* function is defined as

$$sign(x) = \begin{cases} 1 & if \;\; x > 0 \\ 0 & if \;\; x = 0 \\ -1 & if \;\; x < 0 \end{cases}$$

III. PFTC BASED ON NONSINGULAR FAST TERMINAL SLIDING MODE CONTROL (NFTSMC)

Let $x_1 = q \in \Re^n$, $x_2 = \dot{q} \in \Re^n$, in the presence of faults, equation (5) can be rewritten in the state space form as

$$\begin{aligned} \dot{x}_1 &= x_2 \\ \dot{x}_2 &= M^{-1}(x_1)u + f(x_1, x_2) + \Delta(x_1, x_2, u) + \phi(x_1, x_2, u) \\ y &= x_1 \end{aligned} \tag{7}$$

where $u = \tau$ is the control input and y is the output vector.

The design procedure of the NFTSMC consists of two main steps [55-57]. The first step involves constructing the appropriate nonsingular fast terminal sliding mode surfaces, which should have the prescribed desirable dynamical characteristics. The next step is to design a control law that forces the system states to reach the sliding surface in a finite time. For the first step, we let

$$e = x_1 - x_d \tag{8}$$

where $x_d \in \Re^n$ is the desired trajectory.

The sliding surface of the conventional sliding mode control is selected as [41]:

$$s = \dot{e} + \vartheta e, \;\; \vartheta > 0 \tag{9}$$

However, the uses of conventional SMC do not converge to the equilibrium point in finite time because a linear surface is used.

To obtain a finite time convergence, the TSM and NTSM have been developed as follows [47, 49]:

$$s = \dot{e} + k e^{[a]}, \; k > 0, 0 < a < 1 \tag{10a}$$

$$s = e + k' \dot{e}^{[a']}, \; k' > 0, 1 < a' < 2 \tag{10b}$$

The TSM and NTSM converge in a relatively slow rate when far away from the equilibrium point [55]. To enhance the convergence speed, the FTSM is designed by the following differential equation:

$$s = \dot{e} + k_1 e^{[a_1]} + k_2 e^{[a_2]} \tag{11}$$

where $k_1 > 0$, $k_2 > 0$, $a_1 \geq 1$ and $0 < a_2 < 1$. When $a_1 = 1$, (11) has the form of FTSM [49], and (11) coincides with FTSM [48] if there exists positive odd integers v, z satisfying $a_2 = v / z$ with $v < z$. The fast convergence property of (11) can be explained as follows: when the system state stays at a distance from equilibrium, $k_1 e^{[a_1]}$ dominates over $k_2 e^{[a_2]}$, (11) can be approximated by $s = \dot{e} + k_1 e^{[a_1]} = 0$, which guarantees a high convergence rate. When the system state is close to the origin, the term $k_2 e^{[a_2]}$ dominates over $k_1 e^{[a_1]}$, (11) can be approximated by $s = \dot{e} + k_2 e^{[a_2]} = 0$ and determines finite-time convergence. By this way, the dynamics converges very quickly in the whole FTSM (11). However, the control signals contain $e^{a_2 - 1}\dot{e}$, which may cause a singularity to occur if $\dot{e} \neq 0$ and $e = 0$.

Based on the properties of NTSM (10b) and FTSM (11), in this paper, a nonsingular fast terminal sliding mode surface is selected as

$$s = e + \sigma_1 e^{[\varphi]} + \sigma_2 \dot{e}^{[l/p]} \tag{12}$$

where $s \in \Re^n$ is the sliding variable, $\sigma_1 = diag(\sigma_{11}, \sigma_{12}, \ldots, \sigma_{1n}) \in \Re^{n \times n}$ and $\sigma_2 = diag(\sigma_{21}, \sigma_{22}, \ldots, \sigma_{2n}) \in \Re^{n \times n}$ are positive definite matrices, respectively, l and p are positive odd numbers satisfying the relation $1 < l / p < 2$ and $\varphi > l / p$, $e^{[\varphi]} := \left(e_1^{[\varphi]}, \ldots, e_n^{[\varphi]}\right)^T \in \Re^n$, and $\dot{e}^{[l/p]} := (\dot{e}_1^{[l/p]}, \ldots, \dot{e}_n^{[l/p]})^T \in \Re^n$.

For the second step, to ensure that sliding motion occurs and that the error thus converge to zero in a finite time, the derivative of the sliding surface $\dot{s} = 0$ should be satisfied such that

$$\dot{s} = \dot{e} + \sigma_1 \varphi |e|^{\varphi - 1} \cdot \dot{e} + \sigma_2 \frac{l}{p} |\dot{e}|^{(l/p)-1} \cdot \left(\dot{x}_2 - \ddot{x}_d\right) \tag{13}$$

where

$$|e|^{\varphi-1} := diag\left\{|e_1|^{\varphi-1}, \ldots, |e_n|^{\varphi-1}\right\} \in \Re^{n \times n},$$

$$|\dot{e}|^{(l/p)-1} := diag\left\{|\dot{e}_1|^{(l/p)-1}, \ldots, |\dot{e}_n|^{(l/p)-1}\right\} \in \Re^{n \times n}.$$

Substitute (7) into (13), we have

$$\dot{s} = \dot{e} + \sigma_1\varphi|e|^{\varphi-1}\cdot\dot{e} + \sigma_2\frac{l}{p}|\dot{e}|^{(l/p)-1} \cdot\left(M^{-1}(x_1)u + f(x_1,x_2)+\Delta(x_1,x_2,u)+\phi(x_1,x_2,u)-\ddot{q}_d\right) \tag{14}$$

In (14), the total uncertainties take a form of $F(x_1,x_2,u)=\Delta(x_1,x_2,u)+\phi(x_1,x_2,u)$. The following assumption is made:

Assumption 1: There exists a positive constant δ such that

$$\|F(x_1,x_2,u)=\Delta(x_1,x_2,u)+\phi(x_1,x_2,u)\| \le \bar{\Delta}+\bar{\phi}=\delta \tag{15}$$

where $\bar{\Delta}$ and $\bar{\phi}$ are a known upper bound of uncertainties and faults, respectively.

Under the assumption 1 and according to the terminal sliding mode design procedure, a PFTC can be designed as

$$u = u_{eq} + u_{re} \tag{16}$$

where

$$u_{eq} = M(x_1)\left[-\frac{1}{\sigma_2}\frac{p}{l}\left(\dot{e}^{[2-(l/p)]}+\sigma_1\varphi|e|^{\varphi-1}\cdot\dot{e}^{[2-(l/p)]}\right) - f(x_1,x_2)+\ddot{q}_d\right] \tag{17}$$

is used to control nominal component, where $\dot{e}^{[2-(l/p)]} := \left(\dot{e}_1^{[2-(l/p)]},\ldots,\dot{e}_n^{[2-(l/p)]}\right)^T \in \Re^n$

and

$$u_{re} = -M(x_1)\left[\delta+\eta\right]sign(s) \tag{18}$$

is used to compensate for both uncertainties and faults, where $sign(s)=\left(sign(s_1),\ldots,sign(s_n)\right)^T \in \Re^n$. $\eta>0$ is a small constant value. The stability of the system under the PFTC scheme in (16) is demonstrated in Theorem 1.

Theorem 1: Considering the uncertain robot manipulators described in (7) under a faulty condition, the nonlinear sliding surface described in (12), the system trajectory will converge fast to zero within finite time and no occurring of singularity is ensured during the whole process under the controller defined in (16).

Proof: Let the Lyapunov function be $V_1=\frac{1}{2}s^Ts$. Differentiating V_1 with respect to time, we have

$$\dot{V}_1 = s^T\dot{s} = s^T\left[\dot{e} + \sigma_1\varphi|e|^{\varphi-1}\cdot\dot{e} + \sigma_2\frac{l}{p}|\dot{e}|^{(l/p)-1} \cdot\left(M^{-1}(x_1)u + f(x_1,x_2)+F(x_1,x_2,u)-\ddot{q}_d\right)\right] \tag{19}$$

Subtracting (16)-(18) into (19), we have:

$$\begin{aligned}\dot{V}_1 &= s^T\cdot\sigma_2\frac{l}{p}|\dot{e}|^{l/p-1}\cdot\left(\begin{array}{l}F(x_1,x_2,u)\\ -[\delta+\eta]sign(s)\end{array}\right)\\ &\le \sum_{i=1}^{n}|s_i|\cdot\left(\sigma_2\frac{l}{p}|\dot{e}|^{l/p-1}\right)_i\cdot(\delta-\delta-\eta)\\ &\le -\eta\rho(\dot{e})|s|\end{aligned} \tag{20}$$

where

$$\rho(\dot{e}) := \inf_{1\le i\le n}\left\{\left(\sigma_2\frac{l}{p}\left(|\dot{e}|^{l/p-1}\right)\right)_i\right\} \tag{21}$$

Since l and p are odd numbers and $1<l/p<2$, the term $|\dot{e}|^{l/p-1}$ has two possible cases: *i)* $|\dot{e}|^{l/p-1}>0$ for $\dot{e}\neq 0$ and *ii)* $|\dot{e}|^{l/p-1}=0$ only for $\dot{e}=0$. Meanwhile, from (12) for $s\neq 0$, there are also two different cases: 1) $\dot{e}\neq 0$, and 2) $\dot{e}=0$ but $e\neq 0$. For the former case, i.e., $s\neq 0$ and $\dot{e}\neq 0$, there is $\rho(\dot{e})>0$ and $\dot{V}_1<0$. Therefore, for $\dot{e}\neq 0$, the condition for the Lyapunov stability is satisfied. The system will move fast to the sliding mode $s=0$ within finite time.

For the latter case, $s\neq 0$, $\dot{e}=0$ but $e\neq 0$, by substituting (16)-(18) into the second equation of (7), one can obtain

$$\ddot{e} = -\frac{1}{\sigma_2}\frac{p}{l}\left(\dot{e}^{[2-(l/p)]}+\sigma_1\varphi|e|^{\varphi-1}\cdot\dot{e}^{[2-(l/p)]}\right) + F(x_1,x_2,u)-\left[\delta+\eta\right]sign(s) \tag{22}$$

From $\dot{e}=0$, (22) can be rewritten as

$$\ddot{e} = F(x_1,x_2,u)-\left[\delta+\eta\right]sign(s) \tag{23}$$

For both $s>0$ and $s<0$, it is obtained $\ddot{e}<-\eta$ and $\ddot{e}>\eta$, respectively. It is easy to figure out that the system will not always stay on the points ($e\neq 0$ and $\dot{e}=0$). In addition, it is reasonable to assume that there exists a vicinity of $\dot{e}=0$, i.e. $|\dot{e}|\le\xi$ (ξ is a small positive constant) such that $\ddot{e}<-\eta$ and $\ddot{e}>\eta$ for $s>0$ and $s<0$, respectively. Thus, it follows that the crossing of trajectories between two boundaries of the vicinity $\dot{e}=\xi$ to $\dot{e}=-\xi$ for $s>0$ and from $\dot{e}=-\xi$ to $\dot{e}=\xi$ for $s<0$ is executed in finite time, and also the dynamics from the other regions where $|\dot{e}| > \xi$ converges to the boundaries in the finite time [50]. Therefore, it is concluded that the sliding mode $s=0$ can be reached from everywhere in the phase plane, $0-e\dot{e}$, in finite time. In addition, it is also noted that the control (16) does not contain any negative fractional power since $1 < l/p < 2$ and $\varphi > 1$; thus it is singularity-free. Hence, we conclude that from any initial states, the closed-loop system may converge quickly to the origin along NFTSMC (12) in finite time without any singularity. This completes the proof.

Remark 1: When the sliding mode $s=0$ is reached, the system is determined by the nonlinear differential equation: $e+\sigma_1 e^{[\varphi]}+\sigma_2 \dot{e}^{[l/p]}=0$, where $e=0$ is the terminal attractor of the system. The finite time t_s that is taken to travel from $e(t_r)\neq 0$ to $e(t_r+t_s)=0$ is given by [55]:

$$t_s=\frac{\frac{l}{p}|e(t_r)|^{1-\frac{p}{l}}}{\sigma_1(\frac{l}{p}-1)}\cdot F\left(\frac{p}{l},\frac{\frac{l}{p}-1}{(\varphi-1)\frac{l}{p}};1+\frac{\frac{l}{p}-1}{(\varphi-1)\frac{l}{p}};-\sigma_1|e(t_r)|^{\varphi-1}\right) \tag{24}$$

where $F(\cdot)$ denotes Gauss' hypergeometric function. For more details on Gauss' Hypergeometric function, one can refer to the work [67].

IV. AFTC BASED ON TIME DELAY ESTIMATION AND CONTINUOUS NONSINGULAR FAST TERMINAL SLIDING MODE CONTROL

The basic idea of the developed PFTC in (16) is to treat the faulty term $\phi(x_1,x_2,u)$ as an additional uncertainty and organize a control law to compensate for the effect of fault. Although this technique can handle the effects of faults in the system and might achieve stabilization performance, it is a conservative method in that its controllers are designed based on the faulty system without any change in control law even either faults occur or not. Due to the lack of FD information, the control system is designed based on the assumed fault magnitude. The tracking error of the NFTSMC converges to zero if its gain ($[\delta+\eta]$ in (18)) is bigger than the upper bound value of the assumed fault magnitude. However, the upper bound value is difficult to obtain in advance. In addition, if the upper bound value is assumed to be known but big, the sliding gain must be chosen as a big value; unfortunately, this large control gain may cause large chattering on the sliding surface and therefore deteriorate the PFTC system performance. To enhance the performance of the FTC system, we propose an AFTC based on TDE and continuous NFTSMC. The TDE is used here as a robust FD scheme to detect, isolate and estimate the unknown uncertainties and faults. The estimated uncertainties and faults are then used to reconfigure the control system rapidly.

A. Design of a robust fault diagnosis based on time delay estimation (TDE)

Assuming that the uncertainty $\Delta(x_1,x_2,u)$ and fault $\phi(x_1,x_2,u)$ are continuous or piecewise continuous and that the time delay L is sufficiently small, the following approximation is satisfied:

$$\Delta(x_1,x_2,u)_{(t)}\cong\Delta(x_1,x_2,u)_{(t-L)} \tag{25}$$

$$\phi(x_1,x_2,u)_{(t)}\cong\phi(x_1,x_2,u)_{(t-L)} \tag{26}$$

providing an effective estimation of $\Delta(x_1,x_2,u)_{(t)}$ and $\phi(x_1,x_2,u)_{(t)}$, i.e.,

$$\hat{\Delta}(x_1,x_2,u)_{(t)}\triangleq\Delta(x_1,x_2,u)_{(t-L)} \tag{27}$$

$$\hat{\phi}(x_1,x_2,u)_{(t)}\triangleq\phi(x_1,x_2,u)_{(t-L)} \tag{28}$$

where $\hat{\Delta}(x_1,x_2,u)_{(t)}$ and $\hat{\phi}(x_1,x_2,u)_{(t)}$ are the estimation of uncertainty, $\Delta(x_1,x_2,u)_{(t)}$, and fault, $\phi(x_1,x_2,u)_{(t)}$, at the time t, respectively.

From (7) and (27), (28), the TDE can be obtained as:

$$\begin{aligned}\hat{\Delta}(x_1,x_2,u)_{(t)}+\hat{\phi}_{(t)}&\triangleq\Delta(x_1,x_2,u)_{(t-L)}+\phi_{(t-L)}\\&=\dot{x}_{2(t-L)}-f(x_1,x_2)_{(t-L)}-\left(M^{-1}(x_1)u\right)_{(t-L)}\\&=H_{TDE}\end{aligned} \tag{29}$$

where H_{TDE} denotes the time delay estimation.

B. Fault detection and isolation

The proposed TDE-based fault diagnosis observer is able to detect system faults in the presence of uncertainties. The fault diagnosis system must be robust against system uncertainties, but must also be sensitive to any fault. In this paper, the obtained TDE defined in (29) is used as a residual to detect and isolate the faults.

According to (7), $\phi(x_1,x_2,u)=0$ when $t<T_f$. Then, from (29) we have

$$H_{TDE}\triangleq\Delta(q,\dot{q},\tau)\leq\bar{\Delta}=H_{th} \tag{30}$$

By choosing H_{th} as the threshold, the robustness property of the fault detection scheme is guaranteed. A fault is detected and isolated whenever the residual H_{TDE} overshoots its corresponding threshold (H_{th}).

C. AFTC based on TDE and NFTSMC

From (29), the unknown function that includes uncertainties and faults can be described by an estimated TDE H_{TDE} :

$$\Delta(x_1, x_2, u) + \phi(x_1, x_2, u) = H_{TDE} + \varepsilon \tag{31}$$

where ε is the time delay estimation error. From this, the robot dynamics described in (7) can be rewritten as

$$\begin{aligned} \dot{x}_1 &= x_2 \\ \dot{x}_2 &= M^{-1}(x_1)u + H_{TDE} + \varepsilon \end{aligned} \tag{32}$$

Assumption 2: There exist a positive constant $\bar{\varepsilon}$ such that

$$|\varepsilon| \le \bar{\varepsilon} \tag{33}$$

where $\bar{\varepsilon}$ is a known upper bound of time delay estimation error. Based on the analyses in Refs. [18-21], this assumption is reasonable for a sufficiently small L.

For the system (32), the derivative of the sliding surface defined in (13) can be rewritten as

$$\begin{aligned} \dot{s} = \dot{e} + \sigma_1 \varphi |e|^{\varphi-1} \cdot \dot{e} + \sigma_2 \frac{l}{p} |\dot{e}|^{(l/p)-1} \\ \cdot \left(M^{-1}(x_1)u + f(x_1, x_2) + H_{TDE} + \varepsilon - \ddot{x}_d\right) \end{aligned} \tag{34}$$

Based on the derivative of the sliding surface in (34), the AFTC is now designed based on TDE compensation and NFTSMC to accommodate both the uncertainties and faults:

$$u = u_{eq} + u_{TDE} + u_{re} \tag{35}$$

where u_{eq} is designed as the same as (17). And the TDE-based fault compensation term is

$$u_{TDE} = -M(x_1) H_{TDE} \tag{36}$$

and u_{re} is now designed as

$$u_{re} = -M(x_1)\left[\eta + \bar{\varepsilon}\right] sign(s) \tag{37}$$

The stability of the system under the proposed AFTC in (35) is demonstrated in Theorem 2.

Theorem 2: Considering the uncertain robot manipulators described in (7) under a faulty condition, the nonlinear sliding surface described in (12) and the control law defined in (35), the system trajectory will converge fast to zero within finite time and no occurring of singularity is ensured during the whole process.

Proof: Let the Lyapunov function be $V_2 = \frac{1}{2} s^T s$. Differentiating V_2 with respect to time, we have

$$\begin{aligned} \dot{V}_2 &= s^T \dot{s} \\ &= s^T \left[\sigma_2 \frac{l}{p} |\dot{e}|^{l/p-1} \varepsilon - \sigma_2 \frac{l}{p} |\dot{e}|^{l/p-1} \cdot [\eta + \bar{\varepsilon}] sign(s) \right] \\ &\le \sum_{i=1}^{n} |s_i| \left(\sigma_2 \frac{l}{p} |\dot{e}|^{l/p-1} \right)_i (\bar{\varepsilon} - \eta - \bar{\varepsilon}) \\ &\le -\eta \rho(\dot{e}) |s| \end{aligned} \tag{38}$$

Based on (38) and the proof for Theorem 1, we can verify that the origins $s = 0$ of the sliding mode dynamics (34) are globally finite-time-stable equilibrium points and the trajectories of (34) converge to zero in the finite time without singularity under the control law defined in (35). This completes proof for Theorem 2.

Due to the capability of the TDE to estimate a nonlinear function, the TDE error is much smaller than that of its estimation function (uncertainties and faults), i.e, $\varepsilon = \Delta + \phi$. Therefore, $\bar{\varepsilon} = \bar{\Delta} + \bar{\phi} = \rho$, the sliding gain of the AFTC ($\bar{\varepsilon} + \eta$) can be selected as a much smaller value compared with the sliding gain of the PFTC ($\eta + \rho$). Hence, the chattering generated by the AFTC is much smaller compared with PFTC, and hence increasing the performance of the FTC system.

D. AFTC based on TDE and continuous NFTSMC

In the proposed PFTC in (16) and AFTC in (35), chattering is present due to the discontinuity of the *sign* function. In order to eliminate the chattering, we consider the following techniques:

i) The reaching control u_{re} is designed based on a continuous function [49, 57]:

$$u_{re} = -M(x_1)[k_1 s + k_2 s^{[\upsilon]}] \tag{39}$$

where $k_1, k_2 > 0$, $0 < \upsilon < 1$. However, this approach reduces the robustness of the system.

ii) The *sign(s)* function is replaced by a sigmoid function, $\frac{e^{bs} - 1}{e^{bs} + 1}$ [56]. That is the reaching control, u_{re}, is now designed as

$$u_{re} = -M(x_1)\left[\eta + \bar{\varepsilon}\right] \frac{e^{bs} - 1}{e^{bs} + 1},\ b > 0 \tag{40}$$

However, the technique implies deterioration accuracy and robustness.

iii) In this paper, we propose to exploit the HOSM control to eliminate the chattering since this technique not only eliminates the chattering but also increase the accuracy. Unlike other HOSMs, such as the suboptimal algorithm [59-60], the twisting algorithm [61], or the quasi-continuous algorithm [62] is the necessity of using the first time derivative of the sliding variable, the super-twisting (STW) algorithm [63-66] does not require the time derivative of the sliding variable. Thus, we employ it to eliminate the chattering. The reaching control, u_{re}, is now designed as:

$$\begin{aligned} u_{re} &= -M(x_1)[K_1\|s\|^{1/2}\,sign(s) - z] \\ \dot{z} &= -K_2 sign(s) \end{aligned} \tag{41}$$

where K_1 and K_2 are chosen as [66]:

$$K_1 > 2\bar{\varepsilon} \;\text{ and }\; K_2 > K_1 \frac{5k_1 + 4\bar{\varepsilon}}{(2k_1 - 4\bar{\varepsilon})}\bar{\varepsilon} \tag{42}$$

The stability and convergence of the STW algorithm can be proved based on the idea of the design of majorant curves [69] or Lyapunov approach [64-66].

E. Acceleration and velocity estimator

The developed finite time AFTC defined in (35) requires the measurement of position, velocity and acceleration. However, in the robot system defined in (7), only the position measurement is available. Hence, an acceleration and velocity estimator is essential for practical implementation of the controller. The velocity and acceleration signals can be calculated by backward differentiator (BD) technique, as [18-21]:

$$\dot{x}_{1(t)} = \frac{x_{1(t)} - x_{1(t-L)}}{L} \tag{43}$$

$$\ddot{x}_{1(t)} = \frac{x_{1(t)} - 2x_{1(t-L)} + x_{1(t-2L)}}{L^2} \tag{44}$$

However, it should be noted that the measured position signal contains quantization noise due to the employed encoder [68], which when differentiated would induce significant estimation error. To effectively estimate the velocity and acceleration, second-order exact differentiation (SOED) [69] is introduced in this paper:

$$\begin{aligned} \dot{z}_0 &= \upsilon_0, \\ \upsilon_0 &= -\lambda_1 |z_0 - x_1|^{2/3}\, sign(z_0 - s) + z_1 \\ \dot{z}_1 &= \upsilon_1 \\ \upsilon_1 &= -\lambda_2 |z_1 - \upsilon_0|^{1/2}\, sign(z_1 - \upsilon_0) + z_2 \\ \dot{z}_2 &= -\lambda_3 sign(z_2 - \upsilon_1) \end{aligned} \tag{45}$$

Using suitably chosen parameter λ_i, the SOED can achieve

$$z_0 = x_1, z_1 = \dot{x}_1, z_2 = \ddot{x}_1 \tag{46}$$

Remark 2: From (7), the fault estimation can simply be obtained as

$$\Delta(x_1, x_2, u)_{(t)} + \phi_{(t)} = \dot{x}_{2(t)} - f(x_1, x_2)_{(t)} - \left(M^{-1}(q)u\right)_{(t)} \tag{47}$$

This fault estimation can be used to detect and isolate the faults; however, it cannot be used for the design of AFTC defined in (35) because the control input u appears in both sides of (35).

Remark 3: It should be addressed here that the SOED (45) can achieve finite time error convergence no matter what the kind of controller used. This means that the proposed controller and the observer (45) can be designed separately, so that the combined observer-controller output feedback preserves the main features of the controller with the full state available.

Remark 4: From (25) and (26), we can see that the smaller value of L is, the continuous system become and thus the better TDE achieve. In practice, L is chosen as the sampling time. A digital control system behaves reasonably close to the continuous system if the sampling rate is faster than 30 times the bandwidth [70].

Remark 5: The selection of l, p and φ of the proposed nonlinear sliding surface in (12) should satisfy the conditions $1 < l/p < 2$ and $\varphi > l/p$ to obtain fast convergence and no singularity. In general, the relative parameters can be tuned by some adaptive methods [55, 56].

Remark 6: In the developed PFTC in (16), the control system has a fast response with the occurrence of fault since it does not require the fault diagnosis information. However, the proposed AFTC based on the TDE-based fault estimation can compensate the effects of fault rapidly without any time delay due to fault diagnosis. Hence, the proposed AFTC scheme can reduce the time delay between fault occurrence and accommodation. Thus, the proposed AFTC scheme has the advantages of AFTC as well as fast response property of PFTC. In addition, unlike the design of PFTC, the proposed AFTC does not require the prior knowledge of the bound value of fault, which may increases the application capability.

Remark 7: Different from previous FTC approaches [4-8], which do not compensate for the uncertainties in normal operation, although the uncertainties can be compensated when a fault occurs, consequently, the performance of the system in normal operation is reduced, the proposed algorithm developed in this paper can compensate for the uncertainties in normal operation and both uncertainties and faults when a fault occurs.

Remark 8: In practical applications, the encoder signal is always contaminated by noise and the control effort has a chattering. The noise and chattering effects can be amplified by numerical differentiation, which is used to calculate the velocity and accelerator either by using BD ((43) and (44)) or

SOED (45). To reduce the noise and chattering effects, we use a low-pass filter that has the form

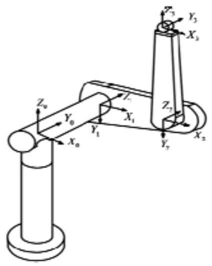

Fig. 1. 3-DOF PUMA robot

$$j\dot{\bar{H}}_{TDE}(t)+\bar{H}_{TDE}(t)=H_{TDE}(t) \tag{48}$$

where j is the filter time constant, and $\bar{H}_{TDE}$ is the output of $H_{TDE}(t)$ after filtration.

V. RESULTS

In order to verify the effectiveness of the proposed FD and FTC algorithms, its overall procedure is simulated for a PUMA560 robot, in which the first three joints are used. The PUMA560 robot is a well-known industrial robot that has been widely used in industrial applications and robotic research. The explicit dynamic model and parameter values necessary to control the robot are given in Ref. [71].

The three degree of freedom (3-DOF) PUMA560 robot is considered with the last three joints locked. A kinematic description of the robot is given in Fig.1. The uncertainties used in this simulation are as follows:

$$F(\dot{q})=\begin{bmatrix}0.5\dot{q}_1+\sin(3q_1)\\ 1.3\dot{q}_2-1.8\sin(2q_2)\\ -1.8\dot{q}_3-2\sin(q_3)\end{bmatrix} \tag{49}$$

and

$$\tau_d=\begin{bmatrix}0.5\sin(\dot{q}_1)\\ 1.1\sin(\dot{q}_2)\\ 0.15\sin(\dot{q}_3)\end{bmatrix} \tag{50}$$

Simulation were conducted in Matlab/Simulink environment by using Runge-Kutta algorithm; the sampling time was set as $10^{-3}s$. Through this simulation, five major contributions of this paper are verified: 1) the use of TDE for fault detection, isolation and estimation; 2) the use of SOED method instead of BD method to estimate the velocity and acceleration; 3) the effectiveness of the proposed AFTC compared to the proposed PFTC; 4) the use of STW algorithm defined in (41) to eliminate the chattering compared to the previous developed methods defined in (39) and (40); 5) the use of NFTSMC defined in (12) compared to the use of NTSMC defined in (10b) and FTSMC defined in (11) for the design of finite time FTC.

A. TDE for fault detection, isolation and estimation

In this section, the capability of TDE for fault detection, isolation and estimation is verified. In order to detect and isolate the faults, the thresholds are first selected. Because the fault diagnosis process does not depend on the type of controller used, we use traditional CTC control as the nominal control for this simulation step. The CTC can be designed as

$$\tau=M(x_1)\left(\ddot{x}_d+K_P(x_1-x_d)+K_V(x_2-\dot{x}_d)+f(x_1,x_2)\right) \tag{51}$$

where the gains $K_p=15I_{3\times3}$, $K_d=10I_{3\times3}$, where $I_{n\times n}$ represents an identity matrix of dimension $n\times n$, are selected. The goal of the control system is to follow the desired trajectory $x_d=[x_{1d},x_{2d},x_{3d}]^T$ with $x_{1d}=\cos(t/5\pi)-1$, $x_{2d}=\cos(t/5\pi+\pi/2)$ and $x_{3d}=\sin(t/5\pi+\pi/2)-1$ as shown in Fig. 3 (dashed blue line). When the robot in normal operation, $\phi(x_1,x_2,u)=0$, TDE is the uncertainty estimation, $H_{TDE}\cong\Delta(q,\dot{q},\tau)$. Fig. 2 show the uncertainty estimation based on TDE. From this figure we can see that the TDE technique give a good capability to estimate an unknown nonlinear function. For this reason, it is used as the residual to detect and isolate the faults. Then, from (30), the thresholds are selected as shown in Fig. 2 (dashed red line). A fault is detected and isolated whenever the residual exceeds its selected thresholds.

To verify the capability of the proposed TDE-based fault diagnosis scheme for fault detection, isolation and estimation, two kind of explicit faults are generated: actuator bias faults and part loss of effectiveness. First, an arbitrary abrupt fault $\delta\tau_1=\left[12(10s),\ 0,\ 0\right]^T$ is generated. It means that we supply a bias fault in the first actuator with the magnitude $12Nm$ at the time $t=10s$. The angle trajectories when the robot in normal operation ($t\le10s$) and when the fault $\delta\tau_1$ ($t>10s$) occurred are shown in Fig. 3. Two observations can be drawn from this figure: 1) under the effect of the fault $\delta\tau_1$, the tracking performance is reduced significantly, and 2) the CTC controller do not compensate for the uncertainties in normal operation and both uncertainties and faults when the fault occurs; consequently, the tracking performance of the system is very low (as shown in Table I and II). The response of the residuals under the effect of the given fault is illustrated in Fig. 4. We can see that only the first residual overshoots the corresponding selected threshold, which indicates that the fault has been occurring in the first actuator. Therefore, it can be concluded that the fault is correctly detected and isolated. Then, we supply an another complex fault $\delta\tau_2=\left[0,\ 20q_1^2+15\dot{q}_1+25\cos(q_1)(10s),\ 0.75u_3(20s)\right]^T$; it means we supply in the second actuator a bias fault

$\delta\tau_{22} = 20q_1^2 + 15\dot{q}_1^2 + 25\cos(q_1)$ at $10s$, and 75% partial loss fault in the third actuator at $20s$. Under the effects of fault

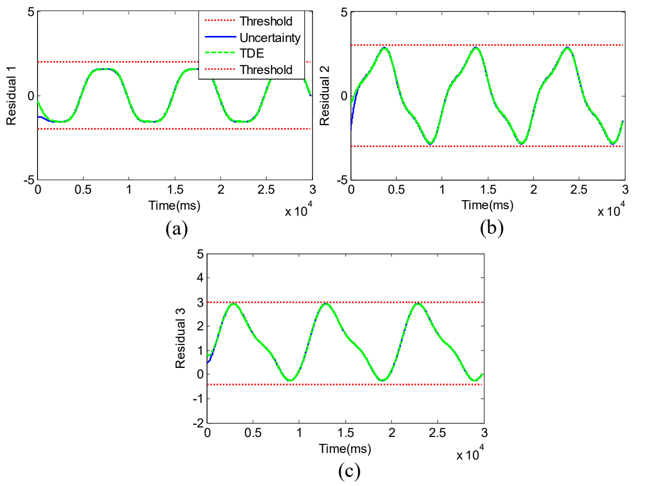

Fig. 2 Residuals of a healthy system and the selection thresholds. (a) Residual 1. (b) Residual 2. (c) Residual 3.

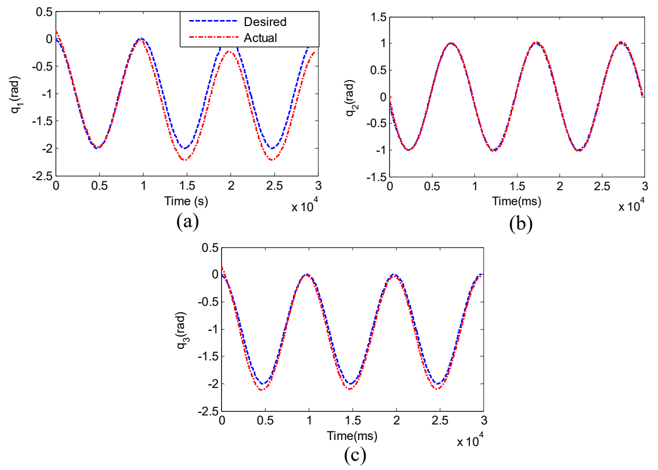

Fig. 3. The desired trajectories and joint angles of the robot manipulator when the actuator fault $\delta\tau_1$ occurs. (a) Joint 1. (b) Joint 2. (c) Joint 3.

$\delta\tau_2$, the tracking performance under CTC is much reduced as shown in Fig. 5. The corresponding responses of the three residuals are shown in Fig. 6. From Fig. 6, we see that the second and third residuals overshoot the corresponding thresholds. Thus, we can conclude that the fault has been detected and isolated successfully.

B. Comparison between BD and SOED for velocity and acceleration estimation

In this section, we compare the performance of the SOED with BD technique in terms of velocity and acceleration estimation. The parameter of BD is selected as $L = 10^{-3}$ (this value is selected as the sampling time) and the parameters of SOED are all set to $\lambda = 5$. The velocity estimation using BD and SOED techniques are shown in Fig. 7. From this figure, it can be seen that the SOED technique give a better performance compared to the BD technique.

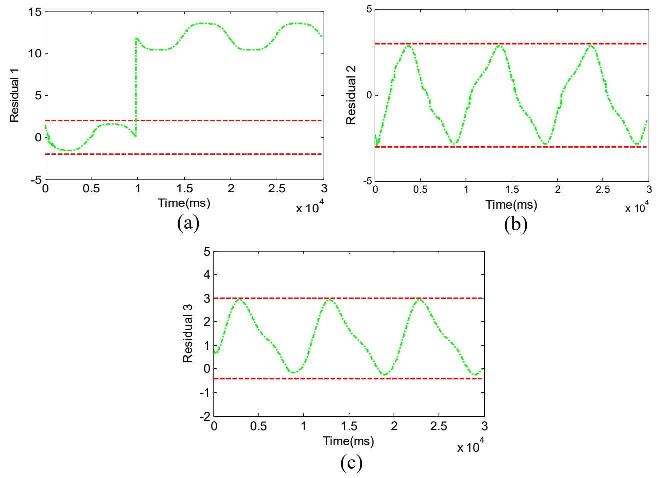

Fig. 4. The response of the residuals of a faulty system under the effect of fault $\delta\tau_1$. (a) Residual 1. (b) Residual 2. (c) Residual 3.

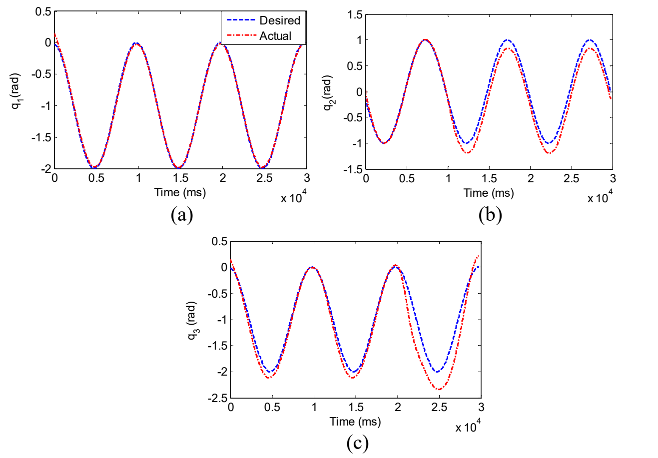

Fig. 5. The desired trajectories and joint angles of the robot manipulator when an actuator fault $\delta\tau_2$ occurs. (a) Joint 1. (b) Joint 2. (c) Joint 3.

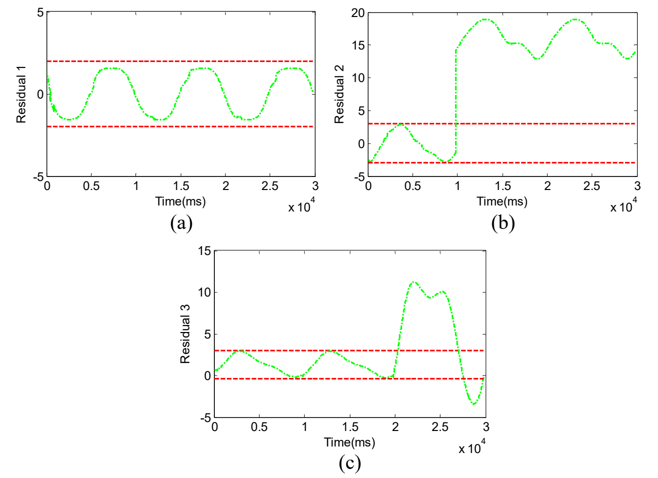

Fig. 6. The response of the residuals of a faulty system under the effect of fault $\delta\tau_2$. (a) Residual 1. (b) Residual 2. (c) Residual 3.

C. Comparison between PFTC and AFTC controllers along with chattering elimination techniques

In this section, the performance of the proposed PFTC and AFTC controllers along with chattering elimination techniques such as super-twisting HOSM algorithm (as defined in (41)), continuous control law (as defined in (39)), and sigmoid approach (as defined in (40)) are compared. That means, we compare the performance of six developed controllers: 1) the proposed PFTC combined with super-twisting HOSM (PFTC- STW), 2) the proposed AFTC combined with super-twisting HOSM (AFTC-STW), 3) the proposed PFTC combined with continuous law (PFTC-Continuous), 4) the proposed AFTC combined with continuous law (AFTC-Continuous), 5) the proposed PFTC combined with sigmoid function approach (PFTC-Sigmoid), and 6) the proposed AFTC combined with sigmoid function approach (AFTC-Sigmoid). These controllers are also compared with the conventional CTC controller. To easily compare the performance of PFTC and

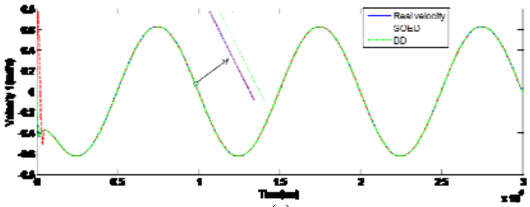

(a)

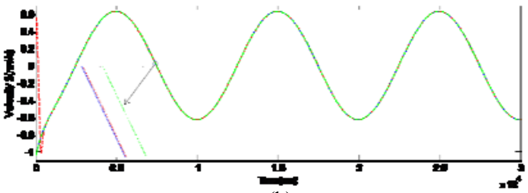

(b)

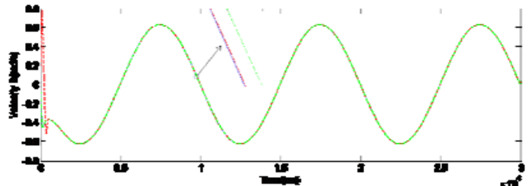

(c)

Fig. 7. Real and estimated velocities using BD and SOED techniques. (a) Joint 1. (b) Joint 2. (c) Joint 3.

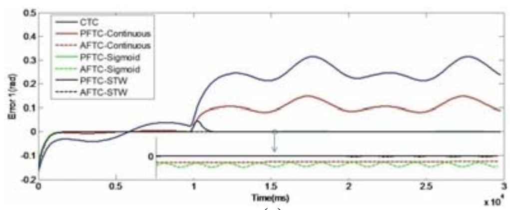

(a)

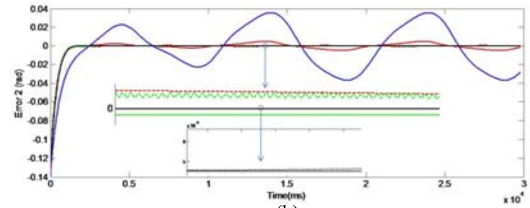

(b)

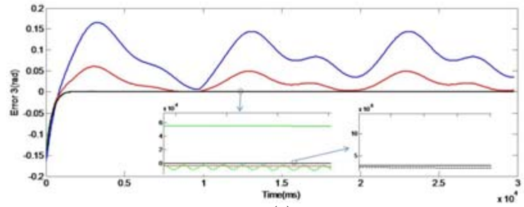

(c)

Fig. 8. Comparison in tracking error among CTC, PFTC-Continuous, AFTC-Continuous, PFTC-Sigmoid, AFTC-Sigmoid, PFTC-STW and AFTC-STW when the actuator fault $\delta\tau_1$ occurs. (a) Error 1. (b) Error 2. (c) Error 3.

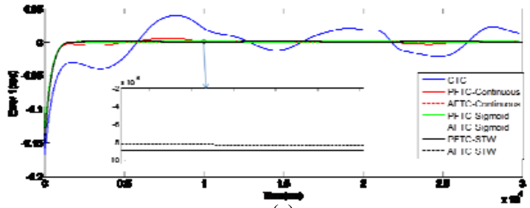

(a)

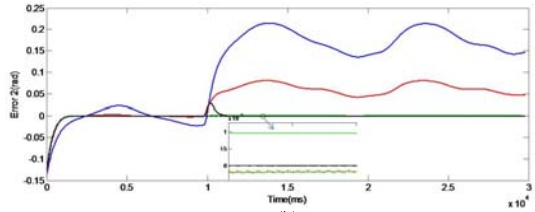

(b)

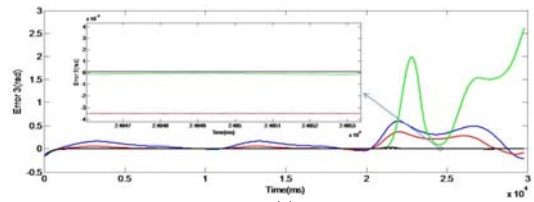

(c)

Fig. 9. Comparison in tracking error among CTC, PFTC-Continuous, AFTC-Continuous, PFTC-Sigmoid, AFTC-Sigmoid, PFTC-STW and AFTC-STW when the actuator fault $\delta\tau_2$ occurs. (a) Error 1. (b) Error 2. (c) Error 3.

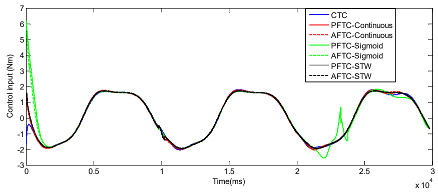

(a)

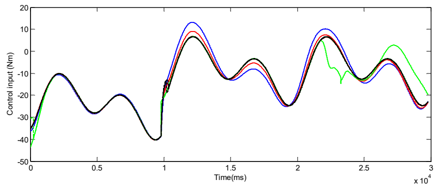

(b)

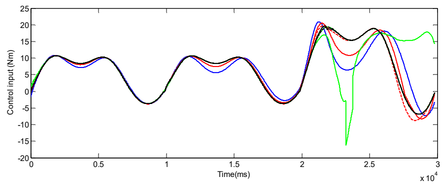

(c)

Fig. 10. Control efforts of the controllers (CTC, PFTC-Continuous, AFTC-Continuous, PFTC-Sigmoid, AFTC-Sigmoid, PFTC-STW and AFTC-STW) when the system under the effect of actuator fault $\delta\tau_2$. (a) Joint 1. (b) Joint 2. (c) Joint 3.

AFTC, the parameters of these controllers are chosen as the same value. In addition, the parameters of the chattering reducing techniques are fairly selected. The parameters of these controllers are selected as $l=9$, $p=7$, $\varphi=1.5$, $\sigma_1 = diag\left(0.8, 0.8, 0.8\right)$ and $\sigma_2 = diag\left(1,1,1\right)$ for NFTSMC, $k_1 = k_2 = 7$ for continuous law approach (defined in (39)), $K_1 = 5$ and $K_2 = 6$ for supper-twisting HOSM approach, and $\rho + \eta = 6$, $b = 1000$ for the sigmoid function approach. The tracking errors of those controllers for the robot system under the faults $\delta\tau_1$ and $\delta\tau_2$ are shown in Figs. 8 and 9, respectively. For easy in comparison, the root mean square error of those controllers for the robot system under the faults $\delta\tau_1$ and $\delta\tau_2$ are also shown in Table I and Table II, respectively. From these figures and tables, two important observations can be given to verify the effectiveness of the proposed algorithm: 1) with the use of TDE for fault diagnosis, the proposed AFTC has a much better performance compared to the PFTC in both fault-free and fault operation; for example: the performance of the AFTC-Continuous is better than the PFTC-Continuous, the AFTC-Sigmoid is better than the PFTC-Sigmoid, and the AFTC-STW is better than the PFTC-STW, and 2) the used of super-twisting HOSM give a better performance compared to the used of continuous law and sigmoid approaches; for example: the performance of PFTC-STW is better than PFTC-Continuous and PFTC-Sigmoid, and the AFTC-STW is better than that of AFTC-Continuous and AFTC-Sigmoid. The smooth control efforts of these controllers for the system under the fault $\delta\tau_2$ are shown in Fig. 10.

D. Comparison between the proposed NFTSMC and NTSMC and FTSMC

In this section, we compare the performance of the AFTC based on the uses of the proposed NFTSMC, the NTSMC (the sliding surface is selected as in (10b)) [47] and the FTSMC (the sliding surface is selected as in (11)) [49]. The super-twisting HOSM algorithm is employed to reduce the

TABLE I

COMPARISON IN ROOT MEAN SQUARE ERROR OF THE CTC, PFTC-CONTINUOUS, AFTC-CONTINUOUS, PFTC-SIGMOID, AFTC-SIGMOID, PFTC-STW AND AFTC-STW WHEN THE ACTUATOR FAULT $\delta\tau_1$ OCCURS

	Link 1	Link 2	Link 3
CTC	0.1764	0.0203	0.0831
PFTC-Continuous	0.0728	0.0024	0.0222
AFTC-Continuous	5.8044×10^{-4}	5.4804×10^{-4}	5.7779×10^{-4}
PFTC-Sigmoid	0.0016	3.9113×10^{-4}	6.3513×10^{-4}
AFTC-Sigmoid	5.2023×10^{-4}	5.1494×10^{-4}	5.2716×10^{-4}
PFTC-STW	0.0015	3.3972×10^{-4}	4.0745×10^{-4}
AFTC-STW	4.3931×10^{-4}	3.4311×10^{-4}	4.0185×10^{-4}

TABLE II

COMPARISON IN ROOT MEAN SQUARE ERROR OF THE CTC, PFTC-CONTINUOUS, AFTC-CONTINUOUS, PFTC-SIGMOID, AFTC-SIGMOID, PFTC-STW AND AFTC-STW WHEN THE ACTUATOR FAULT $\delta\tau_2$ OCCURS

	Link 1	Link 2	Link 3
CTC	0.0191	0.1204	0.1650
PFTC-Continuous	0.0021	0.0423	0.0788
AFTC-Continuous	5.8002×10^{-4}	5.4817×10^{-4}	5.7931×10^{-4}
PFTC-Sigmoid	6.2305×10^{-4}	8.1293×10^{-4}	0.3315
AFTC-Sigmoid	5.2099×10^{-4}	5.1482×10^{-4}	4.7869×10^{-4}
PFTC-STW	4.3993×10^{-4}	8.9438×10^{-4}	0.0020
AFTC-STW	4.3930×10^{-4}	3.4318×10^{-4}	4.3169×10^{-4}

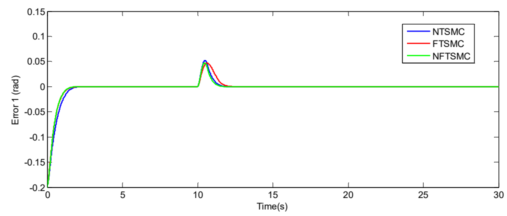

(a)

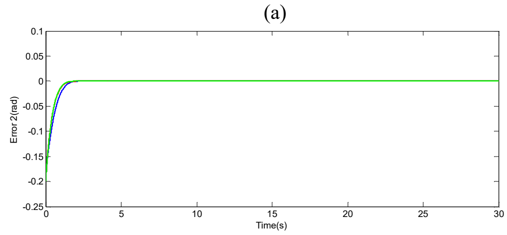

(b)

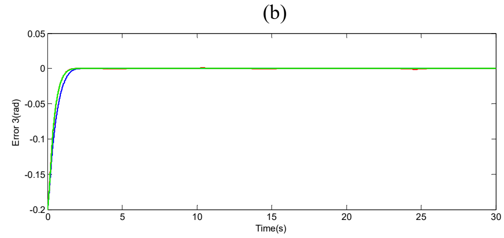

(c)

Fig. 11. Comparison in tracking error among NTSMC, FTSMC, and NFTSMC. (a) Error 1. (b) Error 2. (c) Error 3.

chattering. The tracking errors of these controllers for the robot system when the fault $\delta\tau_1$ occurred are shown in Fig. 11. From Fig. 11, it is obvious to see that all the controllers provided a fast finite time convergent. However, the FTSMC and NFTSMC have a quite similar convergence but have a faster convergence compared to the NTSMC. However, as aforementioned analysis in section III, the FTSMC may meet a singularity problem during operation. Thus, the NFTSMC would be a good choice to design a fast finite time FTC.

VI. Conclusion

A fast finite time AFTC has been developed in this paper for robot manipulator. Comparing with the existing approach, the proposed approach has several significant improvements: 1) Unlike the previous fault diagnosis approaches based on intelligent learning techniques or sliding mode observer, the prosed TDE-based fault diagnosis has a simple and easy in implement and no need for prior knowledge of bound value of fault; 2) Unlike the existing FTC approaches, the proposed AFTC based on NFTSMC guarantees a fast finite time convergence and nonsingular; 3) the proposed approach consider and compensate both the uncertainty and fault in both normal and fault operations; 4) By combining the TDE-based fault estimation and NFTSMC, the proposed FTC scheme possess several advantages over other state-of-the-art approaches such as higher precision, robustness, no singularity, less chattering, fast finite time convergence and no need for prior knowledge of bounded faults. Simulation results for a PUMA560 verify all the mentioned advantages of the proposed strategy.

References

[1] M. Yu, D. Wang, "Model-based health monitoring for a vehicle steering system with multiple faults of unknown types," *IEEE Trans. Ind. Electron.*,vol. 61, no. 7, pp. 3574-3586, 2014.

[2] S. A. Gadsden, S. Yu, S. R. Habibi, "Novel model-based estimators for the purposes of fault detection and diagnosis," *IEEE/ASME Trans. Mechatron.*, vol. 18, no. 4, pp. 1237-1249, 2013.

[3] F. Caccavale, A. Marino, G. Muscio, F. Pierri, "Discrete time framework for fault diagnosis in robotic manipulators," *IEEE Trans. Control Syst. Technol.*, vol. 21, no. 5, pp. 1858-1873, 2013.

[4] A. T. Vemuri, M. M. Polycarpou, and S. A. Diakourtis, "Neural network based fault detection in robotic manipulators," *IEEE Trans. Robot. Autom.*, vol.14, no. 2, pp.12-24, 1998.

[5] K. Patan, "Neural network-based model predictive control: fault tolerance and stability," *IEEE Trans. Control Syst. Technol.*, vol. 23, no. 3, pp. 1147-1155, 2015.

[6] Q. Shen, B. Jiang, P. Shi, C. C. Lim, "Novel neural networks-based fault tolerant control scheme with fault alarm," *IEEE Trans. Cybern.*, vol. 44, no. 11, pp. 2190-2201, 2014.

[7] Q. Song, W. J. Hu, L. Yin, Y. C. Soh, "Robust adaptive Dead Zone Technology for Fault-Tolerant Control of Robot Manipulators Using Neural Networks," *J. Intel. Robot. Syst.*, vol. 33, no. 2, pp. 113-137, 2002.

[8] B. Zhao, Y. Li, "Local joint information based active fault tolerant control for reconfigurable manipulator," *Nonlinear Dyn.*, vol. 77, no. 3, pp. 859-876, 2014.

[9] Q. Shen, B. Jiang, V. Cocquempot, "Adaptive fuzzy observer-based active fault-tolerant dynamic surface control for a class of nonlinear systems with actuator faults," *IEEE Trans. Fuzzy Syst.*, vol. 22, no. 2, pp. 338-349, 2014.

[10] X. Su, P. Shi, L. Wu, Y. D. Song, "Fault detection filtering for nonlinear switched stochastic systems," *IEEE Trans. Auto. Control*, doi: 10.1109/TAC.2015.2465091, 2015.

[11] V. Utkin, *Sliding Modes on control and Optimization*, Springer Verlag, Berlin, Germany, 1992.

[12] Y. Xiong, M. Saif, "Sliding mode observer for nonlinear uncertain systems," *IEEE Trans. Autom. Control,* vol. 46, no. 12, pp. 2012-2017, 2001.

[13] C. Edwards, S. K. Spurgeon, R. J. Patton, "Sliding mode observers for fault detection and isolation," *Automatica*, vol. 36, no. 4, pp. 541-553, 2000.

[14] P. Shi, M. Liu, L. Zhang, "Fault tolerant sliding mode observer synthesis of markovian jump systems using quantized measurements," *IEEE Trans. Ind. Electro.*, vol. 62, no. 9, pp. 5910-5918, 2015.

[15] L. M. Capisani, A. Ferrara, A. Ferreira de Loza, L.M. Fridman, "Manipulator Fault Diagnosis via Higher Order Sliding-Mode Observers," *IEEE Trans. Ind. Electron.*, vol.59, no.10, pp. 3979-3986, 2012.

[16] M. Van, H. J. Kang, Y. S. Suh, K. S. Shin "A robust fault diagnosis and accommodation scheme for robot manipulators," *Int. J. Control, Auto. Syst.*, vol.11, no.2, pp. 377-388, 2013.

[17] M. Van, H. J. Kang, Y. S. Suh "A novel neural second-order sliding mode observer for robust fault diagnosis in robot manipulators," *Int. J. Precision Engineering and Manufacturing*, vol.14, no.3, pp. 397-406, 2013.

[18] K. Youcef-Toumi and O. Ito, "A time delay controller design for systems with unknown dynamics," *Trans. ASME, J. Dyn. Syst. Meas. Control*, vol.112, no.1, pp. 133-142, 1990.

[19] T. C. Hsia, T. A. Lasky, and Z. Gou, "Robust independent joint controller design for industrial robot manipulators," *IEEE Trans. Ind. Electron.*, vol. 38, no.1, pp. 21-25, 1991.

[20] P. H. Chang, J. W. Jeong, "Enhanced operational space formulation for multiple tasks by using time-delay estimation," *IEEE Trans. Robot.,* vol. 28, no. 4, pp. 773-785, 2012.

[21] M. Jin, J. Lee, P. H. Chang, and C. Choi, "Practical nonsingular terminal sliding mode control of robot manipulators for high accuracy tracking," *IEEE Trans. Ind. Electron.*, vol.56, no.9, pp. 3593-3601, 2009.

[22] M. Jin, S. H. Kang, P. H. Chang, "Robust compliant motion control of robot with nonlinear friction using time delay-estimation," *IEEE Trans. Ind. Electron.*, vol.55, no.1, pp. 258-269, 2008.

[23] Z. Gao, C. Cecati, S. X. Ding, "A survey of fault diagnosis and fault-tolerant control techniques Part I: Fault diagnosis with model-based and signal-based approaches," *IEEE Trans. Ind. Electron.*, vol. 62, no. 6, 2015.

[24] J. Jiang, X. Yu, "Fault-tolerant control systems: A comparative study between active and passive approaches," *Annual Reviews in Control*, vol. 36, no. 1, pp. 60-72, 2012.

[25] Q. Shen, D. Wang, S. Zhu, E. K. Poh, "Integral type sliding mode fault tolerant control for attitude stabilization of spacecraft," *IEEE Trans. Control Syst. Technol.*, vol. 23, no. 3, pp. 1131-1138, 2015.

[26] M. Benosman and K. Y. Lum, "Passive Actuators' Fault tolerant control for affine nonlinear systems," *IEEE Trans. Control Syst. Technol.*, vol. 18, no. 1, pp. 152-163, 2010.

[27] R. Wang and J. Wang, "Passive actuator fault-tolerant control for a class of overactuated nonlinear systems and applications to electric vehicles," *IEEE Trans. Vehicular Tech.*, vol. 62, no. 3, pp. 972-985, 2013.

[28] R. Zhang, J. Qiao, T. Li, L. Guo, "Robust fault tolerant control for flexible spacecraft against partial actuator failures," *Nonlinear Dyn.*, vol. 76, no. 3, pp. 1753-1760, 2014.

[29] R. Wang, J. Wang, "Fault tolerant control with active fault diagnosis for four wheel independently driven electric ground vehicles," *IEEE Trans. Vehicular Tech.*, vol. 60, no. 9, pp. 4276-4287, 2011.

[30] A. Paoli, M. Sartini, S. Lafortune, "Active fault tolerant control of discrete event systems using online diagnostics," *IEEE Trans. Vehicular Tech.*, vol. 60, no. 9, pp. 4276-4287, 2011.

[31] H. N. Wu, M. Z. Bai, "Active fault tolerant fuzzy control design of nonlinear model tracking with application to chaotic systems," *IET Control Theory Appl.*, vol. 3, no. 6, pp. 642-653, 2009.

[32] X. Zhang, T. Parisini and M. M. Polycarpou, "Adaptive fault tolerant control of nonlinear uncertain systems: an information-based diagnostic approach," *IEEE Trans. Auto. Control*, vol. 49, no. 8, pp. 1259-1274, 2004.

[33] H. Ferdowsi, S. Jagannathan, "A decentralized fault accommodation scheme for nonlinear interconnected systems," 2013 IEEE Conference on Prognostics and Health Management (PHM), pp.1-6, June 2013.

[34] K. Lim and M. Eslami, "Robust adaptive controller designs for robot manipulator systems," *IEEE J. Robot. Autom.*, vol. 3, no. 1, pp. 54-66, 1987.

[35] W. S. Lu and Q. H. Meng, "Regressor formulation of robot dynamics: computation and applications," *IEEE Trans. Robot. Autom*, vol. 3, no. 1, pp. 54-66, 1987.

[36] S. Y. Yi, M. J. Chung, "A robust fuzzy logic controller for robot manipulators with uncertainties," *IEEE Trans. Syst., Man, Cybern., B, Cybern*, vol. 27, no. 4, pp. 706-713, 1997.

[37] J. Lin, "Hierarchical fuzzy logic controller for a flexible link robot arm performing constrained motion tasks," *IET Control Theory Appl.*, vol. 150, no. 4, pp. 355-364, 2003.

[38] T. C. Hsia, J. Seul, "A simple alternative to neural network control scheme for robot manipulators," *IEEE Trans. Ind. Electron.*, vol. 42, no. 4, pp. 414-416, 1995.

[39] S. S. Ge, C. C. Hang and L. C. Woon, "Adaptive neural network control of robot manipulators in task space," *IEEE Trans. Ind. Electron.*, vol. 44, no. 6, pp. 746-752, 1997.

[40] L. Feng and R. D. Brandt, "An optimal control approach to robust control of robot manipulators," *IEEE Trans. Robot. Autom.*, vol. 14, no. 1, pp. 69-77, 1998.

[41] S. Islam, P. X. Liu, "Robust sliding mode control for robot manipulators," *IEEE Trans. Ind. Electron.*, vol. 58, no. 6, pp. 2444-2453, 2011.

[42] L. Wu, X. Shu, P. Shi, "Sliding mode control with bounded L2 gain performance of makovian jump singular time-delay systems," *Automatica.*, vol. 48, no. 8, pp. 1929-1933, 2012.

[43] A. Sabanovic, "Variable structure systems with sliding modes in motion control- a survey," *IEEE Trans. Ind. Inf.*, vol. 7, no. 2, pp. 212-223, 2011.

[44] D. Bustan, S. K. Hosseini Sani, N. Pariz, "Adaptive fault tolerant spacecraft attitude control design with transient response control," *IEEE/ASME Trans. Mechatron.*, vol. 19, no. 4, pp. 1404-1411, 2014.

[45] Y. W. Liang, S. D. Xu, and C. L. Tsai, "Study of VSC reliable designs with application to spacecraft attitude stabilization," *IEEE Trans. Contr. Syst. Technol.*, vol. 15, no. 2, pp. 332-338, 2007.

[46] S. T. Venkataraman, S. Gulati, "Control of nonlinear systems using terminal sliding mode," *J. Dyn. Sys. Meas. Control*, vol. 115, no. 3, pp. 554-560, 1993.

[47] Z. Man, A. P. Pplinski, H. R. Wu, "A robust MIMO terminal sliding mode controls cheme for rigid robotic manipulators," *IEEE Trans. Autom. Control*, vol. 39, no. 12, pp. 2464-2469, 1994.

[48] X. Yu and Z. Man, "Fast terminal sliding mode control for robot nonlinear dynamic systems," *IEEE Trans. Circuits Syst. I, Fundam. Theory Appl.*, vol. 49, no. 2, pp. 261-264, 2002.

[49] S. Yu, X. Yu, B. Shirinzadeh, Z. Man, "Continuous finite-time control for robotic manipulators with terminal sliding mode," *Automatica*, vol. 41, no. 11, pp. 1957-1964, 2005.

[50] Y. Feng, X. Yu, and Z. Man, "Nonsingular terminal sliding mode control of rigid manipulators," *Automatica*, vol. 38, no. 11, pp. 2159-2167, 2002.

[51] H. Wang, Z. Z. han, Q. Y. Xie, and W. Zhang, "Finite-time chaos control via nonsingular terminal sliding mode control," *Comm. Nonlinear Sci. Numer. Simul*, vol. 14, no.6, pp. 2728-2733, 2009.

[52] M. P. Aghababa, "Finite-time chaos control and synchronization of fractional-order nonautonomous chaotic (hyperchaotic) systems using fractional nonsingular terminal sliding mode technique," *Nonlinear Dyn.*, vol. 69, no. 1, pp. 247-261, 2012.

[53] C. K. Lin, "Nonsingular terminal sliding mode control of robot manipualtors using fuzzy wavelet networks," *IEEE Trans. Fuzzy Syst.*, vol. 14, no. 6, pp. 849-859, 2006.

[54] S. S. Xu, C. Chen, Z. Wu, "Study of nonsingular fast terminal sliding mode fault tolerant control," *IEEE Trans. Ind. Electron.*, vol. 62, no. 6, pp. 3906-3913, 2015.

[55] L. Yang and J. Yang, "Nonsingular fast terminal sliding mode control for nonlinear dynamical systems," *Int. J. Robust Nonlinear Control*, vol. 21, no. 16, pp. 1865-1879, 2011.

[56] H. Li, L. Dou, and Z. Su, "Adaptive nonsingular fast terminal sliding mode control for electromechanical actuator," *Int. J. Syst. Sciences*, vol. 44, no. 3, pp. 401-415, 2011.

[57] J. Zheng, H, Wang, Z. Man, J. Jin and M. Fu, "Robust motion control of a linear motor positioner using fast nonsingular terminal sliding mode," *IEEE/ASME Trans. Mechatron.*, doi: 10.1109/TMECH.2014.2352647, 2014.

[58] G. Edelbaher, K. Jezernik, E. Urlep, "Low-speed sensorless control of induction machine," *IEEE Trans. Ind. Electron.*, vol. 53, no. 1, pp. 120-129, 2005.

[59] G. Bartolini, A. Ferrara, E. Usani, "Chattering avoidance by second-order sliding mode control," *IEEE Trans. Autom. Control*, vol.43, no.2, pp.241-246, 1998.

[60] Ferrara, M. Rubagotti, "A Sub-Optimal Second Order Sliding Mode Controller for Systems With Saturating Actuators," *IEEE Trans. Autom. Control*, vol.54, no.5, pp. 1082-1087, 2009.

[61] G. Bartolini, A. Pisano, E. Punta, an E. Usai, "A survey of applications of second order sliding mode control to mechanical systems," *Int. J. Control*, vol. 76, no. 9/10, pp. 875-897, 2003.

[62] M. Van, H. J. Kang, "Robust Fault tolerant control for uncertain robot manipulators based on adaptive quasi-continuous high-order sliding mode and neural network," *Proc IMechE Part C, J Mechanical Engineering Science*, doi: 10.1177/0954406214544311, 2014.

[63] J. Davila, L. Fridman, A. Levant, "Second-order sliding-mode observer for mechanical systems," *IEEE Trans. Autom. Control*, vol. 50, no. 11, pp. 1785- 1789, 2005.

[64] M. Van, H. J. Kang, Y. S. Suu, K. S. Shin, "Second order sliding mode-based output feedback tracking control for uncertain robot manipulators," *Int. J. Adv. Robot Sys.*, vol. 10, 16:2013, pp. 1-9, 2013.

[65] M. Van, H. J. Kang, K. S. Shin, "Novel quasi-continuous super-twisting high-order sliding mode controllers for output feedback tracking control of robot manipulator, *Proc IMechE Part C, J Mechanical Engineering Science*, doi: 10.1177/0954406214526828, 2014.

[66] H. Khalil, M. Osorio, "A Lyapunov approach to second-order sliding mode controllers and observers," *47th IEEE Conference on Decision and Control*, pp. 2856-2861, 2008.

[67] M. Abramowitz, I. A. Stegun, *Handbook of mathematical functions: with formulas, graphs, and mathematical tables*, Dover: New York, USA, 1972.

[68] J. Zheng and M. Fu, "A reset state estimator using an accelerometer for enhanced motion control with sensor quantization," *IEEE Trans. Control Syst. Technol.*, vol. 18, no. 1, pp. 79-90, 2010.

[69] A. Levant, "Robust exact differentiation via sliding mode technique," *Automatica*, vol. 34, no. 3, pp. 379-384, 1998.

[70] G. F. Franklin, J. Powell, and M. Workman, *Digital control of dynamic systems. Reading*, MA: Addison-Wesley, 1998.

[71] Brian Armstrong, Oussama Khatib, Joel Burdick: "The Explicit Dynamic Model and Inertial Parameters of the PUMA 560 Arm," *IEEE International Conference on Robotics and Automation*, vol. 3, pp. 510-518, 1986.